Journal of Bionic Engineering (2023) 20:543–557
https://doi.org/10.1007/s42235-022-00282-1

RESEARCH ARTICLE

# Design and Realization of a Novel Hybrid-Drive Robotic Fish for Aquaculture Water Quality Monitoring

**Yiting Ji[1,2,3,4] · Yaoguang Wei[1,2,3,4] · Jincun Liu[1,2,3,4] · Dong An[1,2,3,4]**

Received: 6 May 2022 / Revised: 16 September 2022 / Accepted: 29 September 2022 / Published online: 31 October 2022


## Abstract

Thunniform swimmers (tuna) have a swinging narrow sequence stalk and a moon-shaped tail fin, which performs poorly at slow speed, higher acceleration and turning maneuverability. In most cases, faster speed and higher maneuverability are mutually rejection for most marine creatures and their robotic opponents. This paper presents a novel hybrid tuna-like swimming robot for aquaculture water quality monitoring, which interleaves faster speed and higher maneuverability. The robotic prototype emphasizes on streamlining and enhanced maneuverability mechanism designs in conjunction with a narrow caudal propeller to the tail. The innovative design endows the robot to easily execute the multi-mode swimming gait, including forward swimming, turning, diving/surfacing. The capabilities of our robot are validated through a series of indoor swimming pool and field breeding ponds. The robotic fish can achieve a maximum speed up to about 1.16 m/s and a minimum turning radius less than 0.46 Body Lengths (BL) and its maximum turning speed can reach 78.6 °/s. Due to its high speed, maneuverability and relatively small size, the robotic fish shed light on intelligent monitoring in complex aquatic environments.

**Keywords** Hybrid-drive biomimetic robot fish · Water quality monitoring · Multimodal swimming gait

## 1 Introduction

The increasing production of aquaculture is accompanied by the deterioration of water quality. The deterioration of water quality not only leads to environmental pollution but also causes the stunting of breeding objects and even large-scale death. Therefore, it is imperative to strengthen the multi-parameter monitoring of aquaculture water. At present, the commonly used water quality monitoring technologies mostly use fixed-point monitoring methods for local data collection, including portable water quality detectors, online water quality analyzers and water quality monitoring systems based on wireless sensor networks. However, there are too many detection points in aquaculture plants, causing the problem of much manual labor or high cost of detection equipment in existing monitoring technology.

In addition, Autonomous Underwater Vehicles (AUVs) have been widely used in marine environment monitoring as underwater monitoring and control platforms [1]. Traditional underwater vehicle adopts a more mature "propeller" propulsion mode, which has the advantages of simple control, easy replacement and maintenance. However, the currently commonly used AUVs are bulky and heavy and needs to be equipped with a dedicated vessel with complete

Yiting Ji, Yaoguang Wei, Jincun Liu and Dong An have contributed equally to this work.

✉ Yaoguang Wei
wyg@cau.edu.cn

Yiting Ji
jyt@cau.edu.cn

Jincun Liu
liujincun@cau.edu.cn

Dong An
andong@cau.edu.cn

1 National Innovation Center for Digital Fishery, China Agricultural University, Beijing 100083, China

2 Key Laboratory of Smart Farming Technologies for Aquatic Animals and Livestock, Ministry of Agriculture and Rural Affairs, China Agricultural University, Beijing 100083, China

3 Beijing Engineering and Technology Research Centre for Internet of Things in Agriculture, China Agricultural University, Beijing 100083, China

4 College of Information and Electrical Engineering, China Agricultural University, Beijing 100083, China

facilities to handle it, such as moving up and down, which leads to expensive operating costs [2]. In addition, there are many shortcomings, such as low propulsion efficiency, poor maneuverability and poor concealment performance. Over millions of years, fish in nature have evolved excellent physiological structures and extraordinary athletic performance that allow them to cope up with different living conditions through natural selection. And through the use of developed muscles, efficient drag reduction mechanisms and flexible coordination of various fin surfaces, they can swim super fast, have high mobility and have little interference to surrounding marine life.

Robotic fish imitate biological fish in terms of morphology, structure and propulsion methods. According to the main power sources of fish swimming, the propulsion modes can be divided into the following two categories: Body and/or Caudal Fin (BCF)-enabled propulsion and Median and/or Paired Fins (MPF)-enabled propulsion. The former is achieved by swinging of the body and the caudal fins, and the latter is achieved by the wave of the pectoral or dorsal fin to obtain the forward thrust [3]. Since the development of prototypes of underwater bionic vehicles in the 1990s, BCF mode propulsion has received extensive attention. And further subdivided, the BCF mode can be divided into Anguilliform, Subcarangiform, Carangiform and Thunniform according to the proportion of body segments involved in generating propulsion. And the robotic fish behaves differently in each mode [4]. Stefanini et al. [5] developed a 0.99 m-long device using a lamprey as a prototype, which used a muscle-like electromagnetic drive to change the joint angle. Thanks to the design of the multi-segment structure, the highest swimming speed of 0.7 BL/s (Body Length per second) was achieved, which was equivalent to 0.693 m/s, and the minimum turning radius was 0.075 m (equivalent to 0.076 BL). Robotic fish could reach very small turning radius, but the swimming speed was limited. Zhong et al. [6] constructed a wire-pull-driven robotic fish. The rear half of the body was connected by multiple rotating joints and had certain flexibility and elasticity. When the steering gear located inside the head shell drove the wire rope passing through each body segment to move, its tail also swung accordingly. The swimming attitude of the robotic fish could be controlled by the rotation angle and frequency of the steering gear, achieving a maximum direct swimming speed of 0.665 m/s (2.15 BL/s) and a steering rate of 63 °/s. The robotic fish swims faster than the fish itself, but its small body length leads to poor anti-interference ability. The iSplash series of the University of Essex in the United Kingdom, in which the main driving force of iSplash-II [7] came from a motor with a maximum power of 120 W. In addition, so as to guarantee that the robotic fish could swim directly at a certain depth, the head was designed by a servo-controlled pectoral fin for vertical stability. A maximum swimming speed of 3.7 m/s (11.6 BL/s) was achieved at a swing frequency of 20 Hz; however, due to structural design constraints, iSplash-II could not achieve steering. The Tunabot series of robotic fish had outstanding research on the swimming speed. The single-joint driven flexible skinned robotic fish proposed by Zhu et al. [8], when measuring the swimming speed of Tunabot, the experimental results showed that when the motor speed reaches 15HZ, the Tunabot swimming speed exceeds 1.0 m/s (4.0 BL/s); in order to improve the efficiency of the tail fin swing, White et al. [9] proposed the improved version of Tunabot Flex changes the rear part to a multi-joint flexible body and achieves a swimming speed of 4.6 BL/s by selecting new materials and designing a new driving structure. However, this series of robotic fish is designed to pursue the ultimate speed, steering capability is discarded. Du et al. [10] proposed a new dual-joint actuation method for the purpose of solving the direct swimming speed and steering of an underwater bionic platform and applied it to a bionic tuna. The size of the bionic tuna platform was $0.46 \times 0.1 \times 0.13\ m^3$, the weight was 1.8 kg, the maximum instantaneous speed was 0.76 m/s (equivalent to 1.65 BL/s) and the minimum turning radius was 0.35 BL. Robotic fish was not only small, but also slowed to swim. In addition, jet propulsion is also our common propulsion method, which mainly uses liquid ejection to the rear for propulsion. Liao et al. [11] devised a robotic fish with double tail fins, using a double tail fin propulsion mechanism combining tail swing propulsion and jet propulsion. By changing the distance between the two tail fins, the interaction of the tail fins creates eddy currents when they swing, turning them into jets to propel the robotic fish. Although the basic locomotor performance of robotic fish has been successfully implemented, these robotic fish have mainly focused on laboratory studies rather than field studies and practical applications.

So far, some bionic underwater robots have been used for practical tasks, particularly in water quality monitoring. Liang et al. designed AUV SPC-III, a dual-joint biological robot, and successfully carried out a 49 km detection experiment to collect the concentration distribution data of cyanobacteria in Taihu Lake [12], the length of the bionic autonomous underwater vehicle was 1.75 m, and the minimum steering diameter was 5 BL, which meant poor steering maneuverability. Clark et al. proposed an improved multi-objective optimization method for the control of flexible caudal robotic fish for environmental monitoring, underwater structural inspection, hazardous waste and oil spill tracking and live fish behavior studies [13], robotic fish use a flexible caudal fin as the main driving force, but the anti-interference ability is weak. Shen et al. developed a water quality monitoring system based on a robotic dolphin, which consists of setting up monitoring nodes, dynamic robotic nodes and a main

console. Combine fixed and dynamic measurements to obtain water quality parameters such as pH, conductivity, dissolved oxygen and turbidity [14]. It needed to obtain water quality monitoring data through monitoring nodes, and the communication method is complicated. Ryuh et al. proposed a new multi-functional autonomous underwater robotic fish system for marine aquaculture, which is equipped with multiple sensors to monitor multiple water quality parameters such as water temperature, pH value, etc., and can also realize autonomous navigation tasks such as three-dimensional space path planning and obstacle avoidance [15], the robot buoy floating on the water is used as the control center to communicate with a single robot, and the communication method adopted in this paper is relatively complicated. Zhang et al. designed a gliding robotic fish to sample harmful algae concentrations in the Wintergreen Lake [16]. Wu et al. conducted water quality monitoring at the ChanguReservoir (about 3800 m above sea level, which was a very significant reservoir in the Sanjiangyuan National Nature Reserve) in the southeast of Yushu city in the hinterland of the Qinghai-Tibet Plateau [17], the robotic dolphin was 0.74 m long, as well as the actual swimming speed was 0.55 BL/s (0.407 m/s). The size is too small and the swimming speed is slow, and the anti-interference ability in the field is weak. The Boston Engineering Company of the United States has developed the biomimetic robotic fish BIOSwimmer with the shape of a tuna for the Department of Homeland Securit [18]. As a variant of GhostSwimmer [19], the robotic fishtail is equipped with a propeller thruster to generate the thrust required for swimming, and the bionic fishtail is used to assist the propeller to generate the vector thrust required for steering. Through the cooperation of the propeller and the tail, the direct swimming speed of the robotic fish is up to 2.5 m/s, and the turning radius is less than 1 BL. But BIOSwimmer is made of carbon composite material, which is more expensive to use in aquaculture. And the length is about 1.5m, according to its experimental results, the steering maneuverability is not good.

The aim of this paper was to presents a novel hybrid tuna-like swimming robot for aquaculture water quality monitoring. The robot prototype features a streamlined fuselage modeled on a tuna with enhanced maneuverability mechanisms, as well as a narrow rear propeller. The innovative robot enables a multimodal swimming gait including forward stroke, turn, dive and surfacing. In addition, our designed robotic fish is equipped with multiple sensors, enabling it to collect depth and attitude data of the robotic fish and perform water quality monitoring tasks. Finally, to verify the feasibility of the biomimetic system designed for water quality monitoring, we conducted extensive aquatic experiments in the field. Among them, the main contributions are summarized as follows:

- Faster speed. Propeller propulsion enhances the anti-interference ability of the robotic fish and better adapts to the wild wind and wave environment.
- Higher maneuverability. The double-joint fish-like propulsion method of the waist and tail makes the robot fish have strong steering ability.
- Little disturbance to fish environment. Pectoral fins or body swings can reduce the disturbance to the fish in the environment of high fish breeding density.

The reminder of the paper is organized as follows: Section 2 describes the overall mechatronic design and hardware architecture of hybrid-driven robotic fish. In Section 3, the multimodal swimming gait is presented. In Section 4, the experimental results of multi-modal motion and water quality monitoring are presented. Finally, Sect. 5 provides conclusions and future work.

## 2 Overview of the Hybrid-Driven Robotic Fish

### 2.1 Mechanism Design

We hope to transform existing technical equipment by learning and imitating the morphological structure and swimming mechanism of fish so as to explore and create a new underwater vehicle featuring high speed, high mobility, high concealment and low disturbance. As illustrated in Fig. 1a, we propose a mechanical structure of a hybrid-driven robotic fish for water quality monitoring, and the robotic fish's prototype is depicted in Fig. 1b. The tuna-shaped streamline design is adopted to reduce the resistance of fluid resistance. The conical head and the spindle-shaped body can provide sufficient internal load space, which is conducive to the installation of various devices while facilitating machining. Due to the fixed dimensions of electrical modules such as components, motors and various sensors, and considering the above factors, the overall size of the designed bionic tuna is about 1 m, as shown in the Fig. 1c, d. The fin surfaces of the pectoral fin, dorsal fin and caudal fin are all low-speed airfoil NACA-0018 of NACA series, with a relative thickness of 18%, which can reduce water resistance. The shell material is the polyoxymethylene engineering plastic POM known as "Saigang". POM is a kind of engineering plastic with excellent performance. It has excellent properties such as high strength, good elasticity, wear resistance, heat resistance and impact resistance. It has a small friction coefficient, is not easy to absorb water and has good self-lubrication and fatigue resistance.

In terms of mechanical structure, the hybrid-driven robotic fish consists of four parts: head, body, waist and tail. As showed in Fig. 2a, the head of the robotic fish is

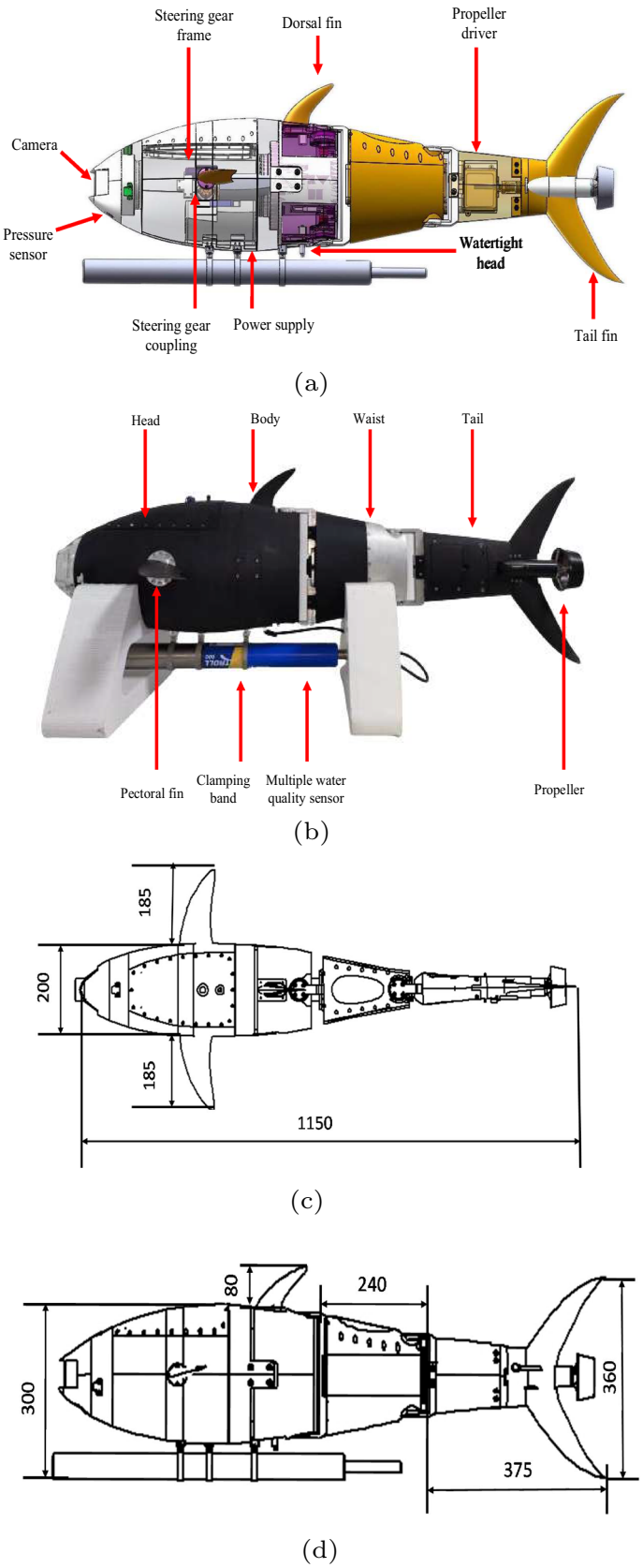


**Fig. 1** Mechanical design of the conceived robotic fish. **a** Mechanical design, **b** robotic fish's prototype, **c** top view of bionic tuna outline structure and dimensions, **d** front view of bionic tuna outline and dimensions

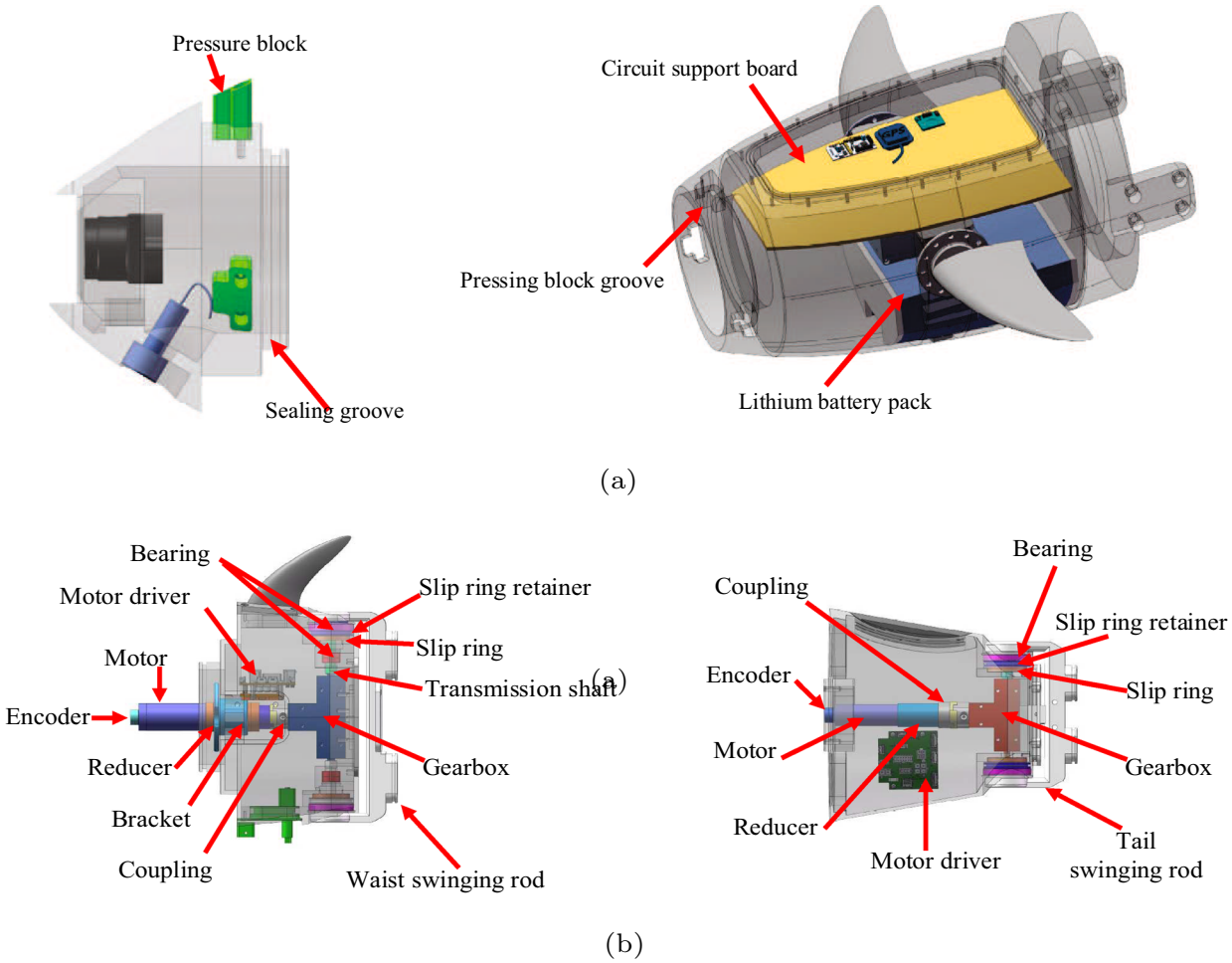


**Fig. 2** Integrated dynamic seal mechanism. **a** Mechanism of the head, **b** internal structure of waist and tail

detachable and is divided into a front end and a rear end. The front end imitates the conical head of the tuna, and the transparent cabin design of the head of the bionic tuna is made of acrylic material (Polymethylmethacrylate, PMMA) with a thickness of 3 mm. Acrylic material can ensure pressure resistance under water, and at the same time, it has good light transmittance, and a camera and pressure sensor are designed inside. The front shell is designed with a slot that is fixed and sealed with the rear shell through a pressure block, and there are three pairs of seals along the sealing ring. Due to the limited internal space of the bionic tuna, the design of its pectoral fin structure cannot be overly complicated. The pectoral fin compartment of the bionic tuna is located behind the transparent compartment, between the circuit support plate and the lithium battery pack. The bionic tuna has a pair of pectoral fins with two degrees of freedom to meet the internal space constraints of the bionic tuna and its design needs. Each pectoral fin is driven by a servo, and the two servos are symmetrically fixed on the head shell through the pectoral fin bracket. Since the pectoral fins are located outside the fish body and need to be rotated, the rudder inside the fish body is driven by a transmission shaft. The machine is connected to the external pectoral fins to complete the transmission. In order to facilitate the maintenance of damaged internal components, the rear end of the robot fish head adopts a detachable casing top cover design to facilitate the adjustment of the internal structure of the bionic tuna, and the fluororubber O-ring is used for static sealing at the connection. The dorsal fin of the bionic tuna is an inactive fin surface fixed on the back of the robotic fish. The connection between the dorsal fin and the shell is statically sealed with a fluororubber O-ring, and is fixed on the top of the shell by screws. The main function of the dorsal fin is to passively maintain the stability of the bionic tuna heading, while maintaining the overall streamline of the bionic tuna.

The waist joint drive module is composed of waist joint motor, driver, encoder, reducer, coupling, gearbox, transmission shaft, waist swinging rod, etc. The module uses T-rings at the slip ring for dynamic sealing. The structure

of the waist joint compartment is shown in the Fig. 2b. After receiving the motion control command, the main controller controls the motor driver to drive the motor output shaft to rotate. At the same time, the motor output shaft drives the entire tail joint compartment to swing through the gearbox and the transmission shaft. The tail joint compartment is located behind the waist swinging rod, and the tail joint motor, encoder, reducer, coupling, driver, gearbox, transmission shaft and other components are installed inside, and T-ring is used for dynamic sealing at the slip ring. The tail joint compartment is driven by the driver to rotate the motor, and the output shaft drives the tail fin to swing. The structure of the tail joint compartment is shown in the Fig. 2b. A fluororubber O-ring is used for static sealing at the connection between the cover and the housing. The propeller control cabin is located at the tail fin of the bionic tuna. Based on the design of the tail fin of the tuna, the propeller is integrated to improve the mechanism. The driver receives the motion control command from the main control cabin and drives the propeller to rotate according to the rotation direction and rotation speed required in the control command.

The ultimate robot is about 1.15 m long and weighs about 19 kg. Table 1 lists the basic technical parameters of the developed hybrid-driven robotic fish.

**Table 1** Technical parameters of the developed hybrid-driven robotic fish

| Items | Characteristics |
|---|---|
| Size ($L \times W \times H$) | $\sim 1.15 \times 0.562 \times 0.393\ \mathrm{m}^3$ |
| Total mass | ~ 19 kg |
| Number of the motor | 4 |
| Drive mode | Coreless and DC brushless motors |
| On-board sensors | Pressure sensor, inertial sensor, GPS |
| Power supply | DC 24 V |
| Operation time | ~ 4 h |
| Controller | STM32F407 (ARM based) |
| Data storage mode | SD card in STM32F407 |
| Communication module | E62-433T20D (433 MHz) |
| Inertial sensor | JY901 |
| Pressure sensor | MS5837 |
| Maximum swimming speed | 1.153 m/s (1 BL/s) |
| Maximum turning rate | 78.6 °/s |
| Minimum turning radius | 0.53 m (0.46 BL) |

## 2.2 Hardware Architecture

The hardware architecture of the hybrid-driven robotic fish is shown in Fig. 3. The STM32F407 microcontroller with high performance and low power consumption is used as the core controller to handle various functional interfaces, which is equipped with multiple sensors. These include pressure sensors to get the depth of the robotic fish in the water, GPS to get its current position, inertial sensors to get its attitude and multiparameter water quality sensors to monitor changes in temperature, dissolved oxygen and pH. A PC is used as the main console of upper computer, which is mainly responsible for data processing, data dynamic display and advanced motion control of robotic fish. A wireless communication module, E62, is used for data interaction between the robot fish and the upper computer console, including issuing control commands and receiving data collected by multiple sensors. Therefore, the embedded system enables the robot not only to input data from external sensors, but also to control the movement mode of the robotic fish.

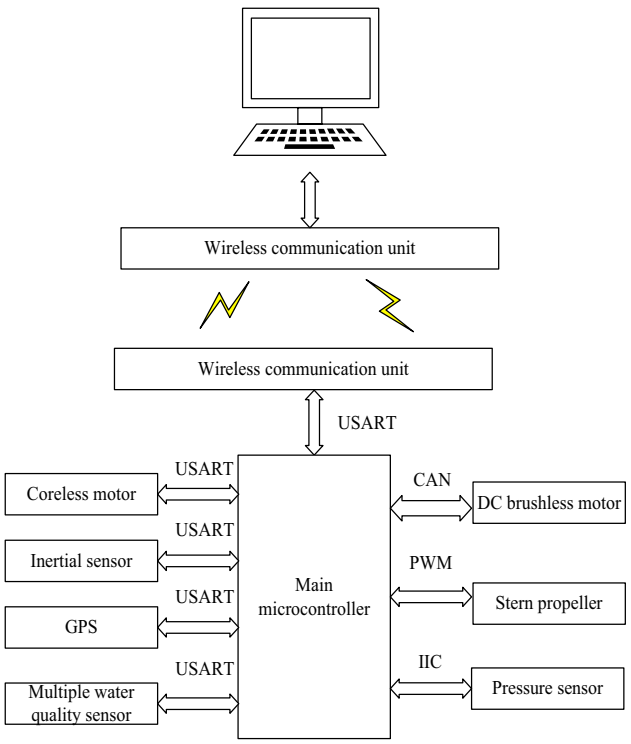


**Fig. 3** Hardware architecture of the robotic fish

# 3 Multimodal Swimming Gaits

Fish mainly oscillate their body or a part of the body to create a pressure difference on the surface of the fish's body. This pressure differential is the main driving force for the fish to swim forward. Among them, the tuna swimming forward power is all provided by the swing of the tail. The tail of this type of fish tends to look very powerful, and the body is in an ideal streamlined shape. The thickest part of the body appears two-fifths of the back from the head, making

this type of fish very suitable for long-distance trekking. In this paper, traditional propellers are used instead of tail swing and combined with pectoral fins and lumbar-tail joints for driving, so as to improve the maneuverability and anti-interference ability of the robotic fish. It can provide multi-modal swimming gait for the robot, like forward swimming, turning maneuvers and submerging/ascending.

### 3.1 Forward Swimming

The forward swimming can be realized by swinging the pectoral fins, i.e., MPF mode, which is shown in Fig. 5a. It can also be finished by swing of the body's waist and tail joints, i.e. BCF model, which is presented in Fig. 5b. Furthermore, the propulsion of the tail propeller, which is illustrated in Fig. 5c, can provide high-thrust. CPG (central pattern generator) is a neural circuit found in invertebrates and vertebrates that can generate periodic motor commands without sensory feedback. The CPG has been proven and widely used to generate the desired swimming gait. As the key of CPG model, Hopf oscillator can be used to achieve coordinated motion control between multiple joints. Among them, the pectoral fin CPG outputs the pectoral fin control signal and outputs it to the left and right pectoral fin servos, respectively, through the conversion function; the waist and tail CPG units have a coupling relationship. Finally, the tail thrusters pass through controlled by a single parameter. The specific equation is as follows:

$$\begin{cases} \dot{x} = -\omega y + x\left(m - x^2 - y^2\right) \\ \dot{y} = \omega x + y\left(m - x^2 - y^2\right), \end{cases} \tag{1}$$

where $x$ and $y$ represent the state variables of the pectoral fin CPG unit; $\omega$ represents the frequency of the CPG output signal, which is used to characterize the period, and the calculation formula is $T = 2/\pi\ \omega$; m is the amplitude of the CPG output signal; and $\dot{x}$ and $\dot{y}$ are the first-order differentials of x and y, and both are intermediate quantities.

$$\begin{cases} \dot{x}_i &= -\omega_i y_i + x_i(m_i - x_i^2 - y_i^2) + h_1\left(x_{i-1}\cos\varphi_i + y_{i-1}\sin\varphi_i\right) \\ \dot{y}_i &= \omega_i x_i + y_i\left(m_i - x_i^2 - y_i^2\right) + h_2\left(x_{i+1}\sin\varphi_i + y_{i+1}\cos\varphi_i\right), \end{cases} \tag{2}$$

where $x_i$ and $y_i$ are the oscillation states of the $i$-th oscillator, when $i = 0, 1$, respectively, waist and tail CPG units; $x_i$ and $y_i$ represent state variables, respectively, $x_i^2$ and $y_i^2$ represent the differentiation of state variables, $\omega_i$ is the frequency of the CPG output signal, $m_i$ is the amplitude of the output signal, $h_1$ is the coupling coefficient of the waist CPG to the tail CPG, $\varphi_i$ is the phase difference of the CPG signal and $h_2$ is the coupling coefficient of the tail CPG to the waist CPG. By setting parameters, the output signals of the left and right pectoral fins, waist and tail joints of the CPG unit are shown in Fig. 4a, b.

The ordinate of each point marked in the figure corresponds to the angle value of the joint. When the PC sends a control command to adjust the swing amplitude and frequency of the joint, the CPG output signal is transformed by modifying the parameters $\omega$ and $m$. The pectoral fin servo and the waist and tail joint motors are all driven and controlled by the "(absolute) position control mode", so it is necessary to convert the output angle value into the corresponding (target) position value proportionally to drive the pectoral fin servo or waist/tail joint motors to the target position. The conversion formula is as follows:

$$\begin{cases} \text{Position 1} = \text{Angle 1} \times 2048/180 + C \\ \text{Position 2} = \text{Angle 2} \times 1000, \end{cases} \tag{3}$$

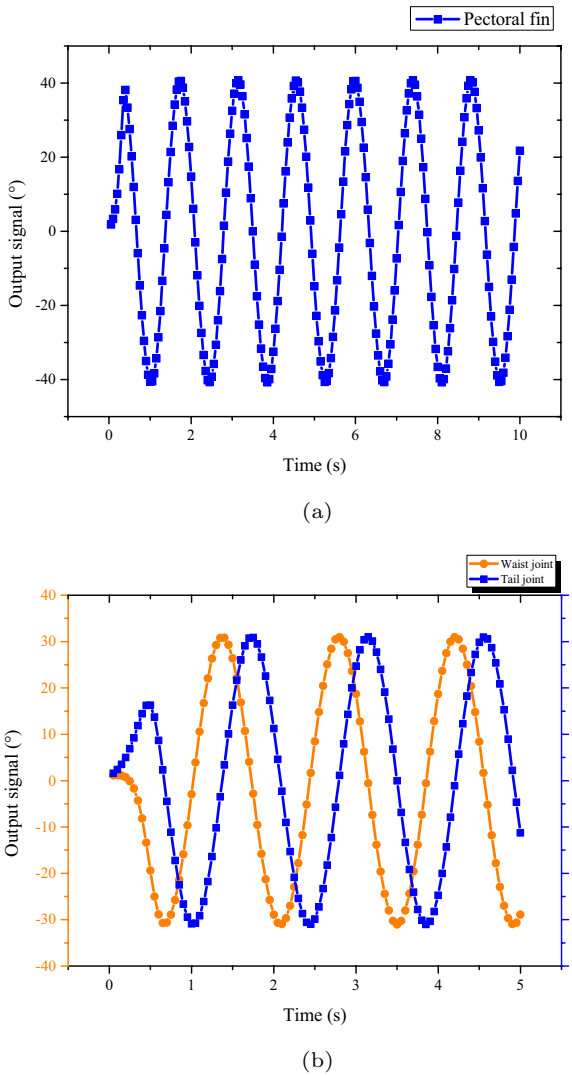


**Fig. 4** CPG output signal diagram. **a** Left and right pectoral fins CPG output signals, **b** waist and tail joints CPG output signals

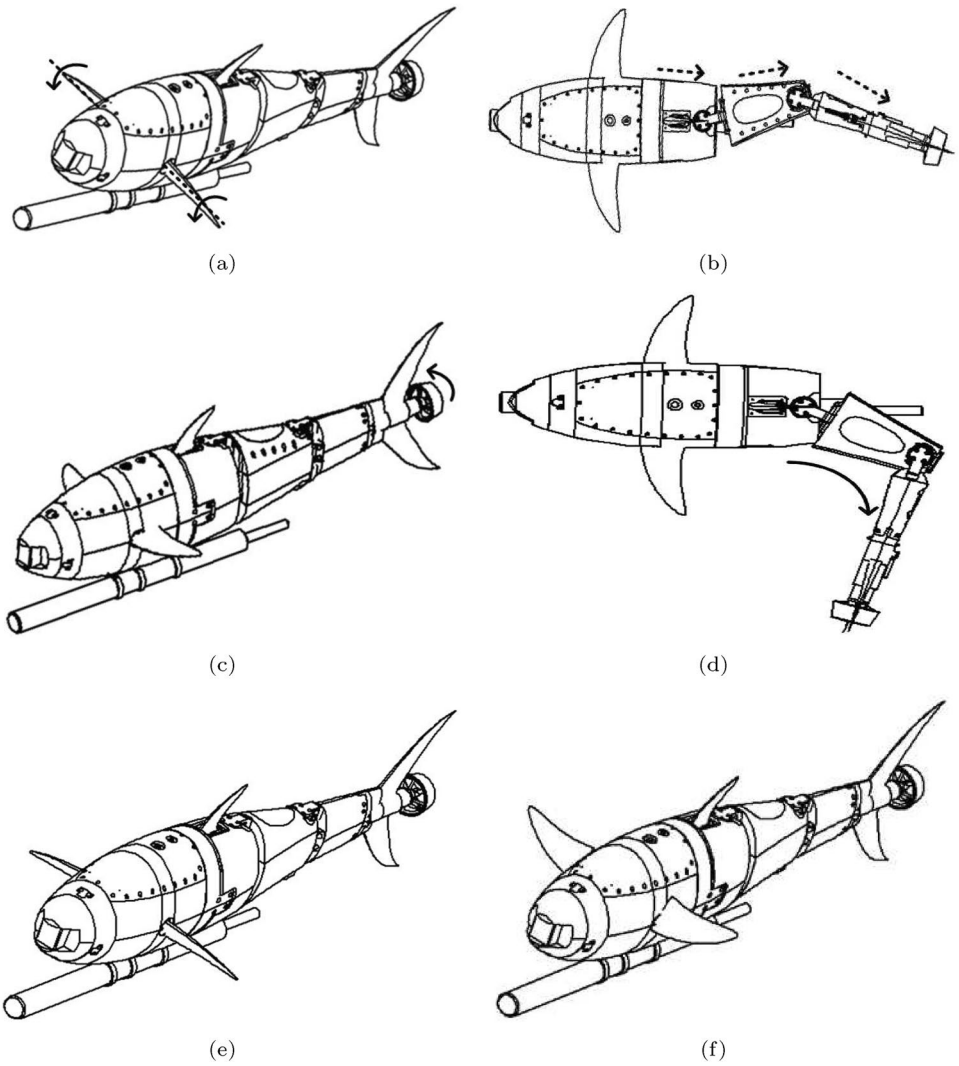


**Fig. 5** Multiple locomotor patterns. **a** Swimming forwards through MPF mode, **b** swimming forwards through BCF mode, **c** swimming forwards through the propulsion of the tail propeller, **d** turning left, **e** submerging, **f** ascending

where Position 1 is the position value of the pectoral fin servo, Angle 1 is the angle value output by the pectoral fin CPG model, $C$ is the corresponding center position when the pectoral fins swing. Position 2 is the position value of the waist/tail joint motor, and Angle 2 is the angle value output by the waist/tail joint CPG model.

$$\{P\} = k\omega + \text{bias}, \tag{4}$$

where $\omega$ is the frequency of the aforementioned CPG control signal, k is the proportional coefficient and bias is the offset. The output P is the duty cycle of the motor PWM control signal.

### 3.2 Turning Maneuvers

The rotational motion in the horizontal plane can be achieved in a variety of ways: for example, pivot steering is achieved by flapping both pectoral fins with different angle of attack errors [20], using its tail fin to achieve steering motion, and the C-shaped sharp turn is realized by swinging the waist–tail joint in the same direction by a certain amount of amplitude and so on. The multi-joint BCF turning movement is relatively smooth and effective [21–24], the reason is that the multi-joint BCF propulsion method can use the agile body and tail fin of the robotic fish to produce a C-shaped turning. As shown in Fig. 5d. In order to achieve a faster turning rate on the premise of ensuring smooth steering, the robotic fish rotates the waist-tail joint motor to the limit position in the same direction. At the same time, the driving motor of the tail propeller rotates clockwise and drives together, helping the robotic fish to carry out turn.

### 3.3 Submerging/Ascending

One common conclusion is that the dynamic lift (pitch moment) helps robotic fish swim up or down. For example,

placing a buoyancy adjustment mechanism on the robotic fish's head, the slight weight change of slowly dragging the piston may result in a larger pitching moment [25]; or the pectoral fin is offset to a certain angle, and the required propulsion is generated through the movement of the rear body [26]. The robotic fish designed in this paper uses a different method to submerge/ascend. The pitching motion of the proposed robotic fish is realized by two independent pectoral fins, driven by propellers. It can be shown in Fig. 5e, f. by applying the offset of the two pectoral fins between 0 ° and 90 ° (or − 90 °) and generate thrust through the rotation of the propeller so that the robot will submerge (or ascend). Therefore, the robot can swim in 3D.

## 4 Experiment and Results

In order to verify the swimming performance of the proposed mechatronic design, a large number of experiments are carried out. Specifically, these experiments mainly include two groups, the indoor swimming pool experiment for analyzing the motion performance of robotic fish and the practical application experiment of farmer's pond for water quality monitoring.

### 4.1 Experimental Setup

The indoor experiments were conducted in a swimming pool with a length of 23 m, a width of 3 m and a depth of 1.8 m. In order to effectively verify the propulsion performance of the hybrid-drive robotic fish. In particular, some marks were added to assist in detecting the movement performance. Multi-sensor data (equipped with multiple on-board sensors including pressure sensors, inertial sensor, and GPS) was stored on the single-chip SD card, which cloud more accurately estimate the speed and attitude of the hybrid-driven robotic fish.

### 4.2 Swimming Speed Tests

At the beginning of the experiment, the direct swim speed was first tested. Several experiments showed that the swimming speed of MPF was 0.058 m/s, the swimming speed of BCF was 0.144 m/s. The tail thruster was used for propulsion by processing the sequence images and measurement data taken by the camera; the swimming speed and stability of the robot could be demonstrated. In the experiment, the swimming speed of the robot according to various swimming parameters (propeller PWM pulse duty cycle speed regulation) was tested. It is shown in Fig. 6a, from the test results that the swimming speed reaches the highest when the propeller is advancing at full speed. The maximum swimming speed was 1 BL/s (1.153 m/s). Fig. 6b shows the instability of the robot's BCF motion mode during swimming, the maximum yaw angle for BCF propulsion is 16.45 °, and the average angle is 3.74 °. The maximum yaw angle for propeller propulsion is 4.79 °, and the average angle is 0.55 °. It can be clearly concluded that propeller propulsion has higher stability than BCF propulsion during swimming. In environmental exploration or surveillance, the stability of the robotic fish's body during swimming plays a very considerable role in whether the camera placed on the robotic fish's head can capture clear and stable images.

### 4.3 Turning Maneuvers Tests

Extensive repeated tests have been executed to assess the turning maneuvers of the hybrid driven robotic fish. In each

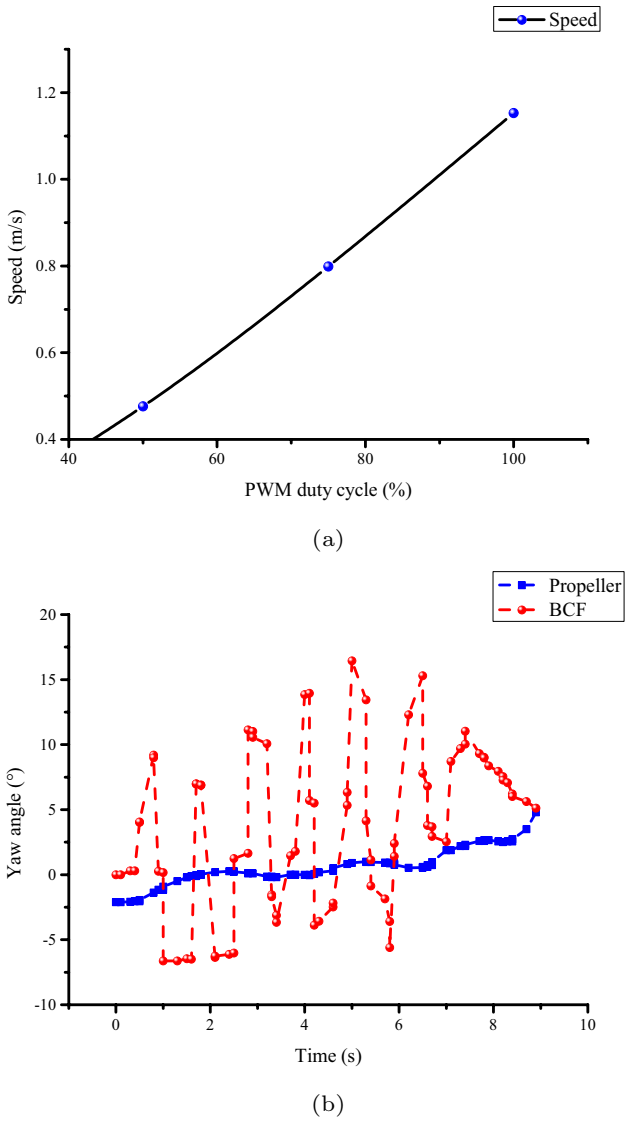


**Fig. 6** Swimming speed tests of the robotic fish. **a** Swimming speed, **b** yaw angle of robotic fish in different propulsion modes

experiment, the robot remained stationary and turned left/right, continuously yawing. For cornering performance testing, the following two important metrics are usually included: (1) turning radius and (2) turning rate. Fig. 7a showed a snapshot sequence of a left turning motion, as well as the measured yaw angle and turning rate shown in Fig. 7b. The robot could complete left and right rotations in 4.6 s and 4.2 s. At the same time, the angular velocity and yaw angle data were stored in the SD card, which means that the average rotation rate was about 78.6 °/s. After many test experiments, the measured turning radius was about 0.53 m (about 0.46 BL).

### 4.4 Submerging/Ascending Tests

The ability of swimming robot to submerge/ascend was the linchpin to achieve 3D mobility. To evaluate the performance of propeller, the propellers and pectoral fins of the robotic fish were used for a series of three-dimensional space movement experiments. The former was used to reach a certain propulsion speed, while the latter was used to produce pitching moments under the action of propulsion speed. Several snapshots of a whole process of submerging and ascending motions is shown in Fig. 8a. When the robotic fish needs to complete the motions of

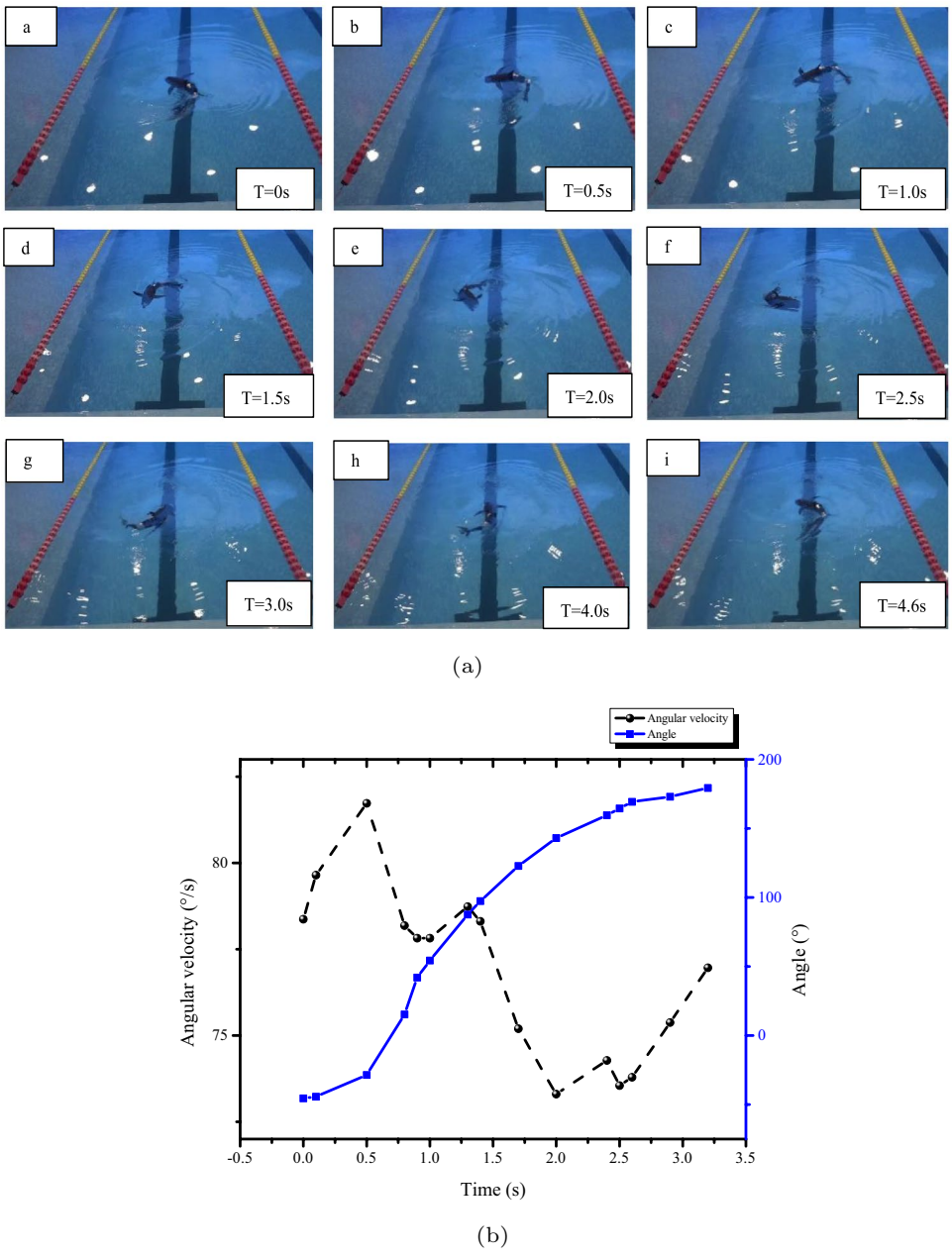


**Fig. 7** Turning maneuvers tests of the robotic fish. **a** Snapshot of the turning left motions, **b** the robotic fish of left turning rate and angle

autonomous submerging and ascending, the maximum submerging depth is set to 1.4 m. The robotic fish started to dive by adjusting the rotational angle of the pectoral fins to 45 ° and advancing the propeller. At the same time, the pitch angle of the robotic fish's body increased toward the bottom of the pool. When the pressure sensor at the fish head senses that the water depth reached 1.4 m, the main control board immediately sent an instruction to rotate the pectoral fins to − 45 ° so that the robotic fish began to ascend. During this movement, the depth and pitch data required for analysis are stored on the SD card. According to the data collected by the inertial sensor, the change of the pitch angle with the change of depth is displayed in Fig. 8b, the complete process of the attitude change of the robotic fish is demonstrated. Specifically, the pitch angle of the robotic fish first increased with the depth, and when $t = 7.4$ s, it reached the maximum pitch angle of about 20.099 °, and its diving speed reached 0.19 m/s. Next, the ascending motion was followed. At the beginning of ascending, the robotic fish started to ascend by adjusting the rotation angle of the pectoral fin to − 45 °. In short, thanks to the pectoral fins and propellers, the robotic fish successfully performed expected submerging and ascending motions.

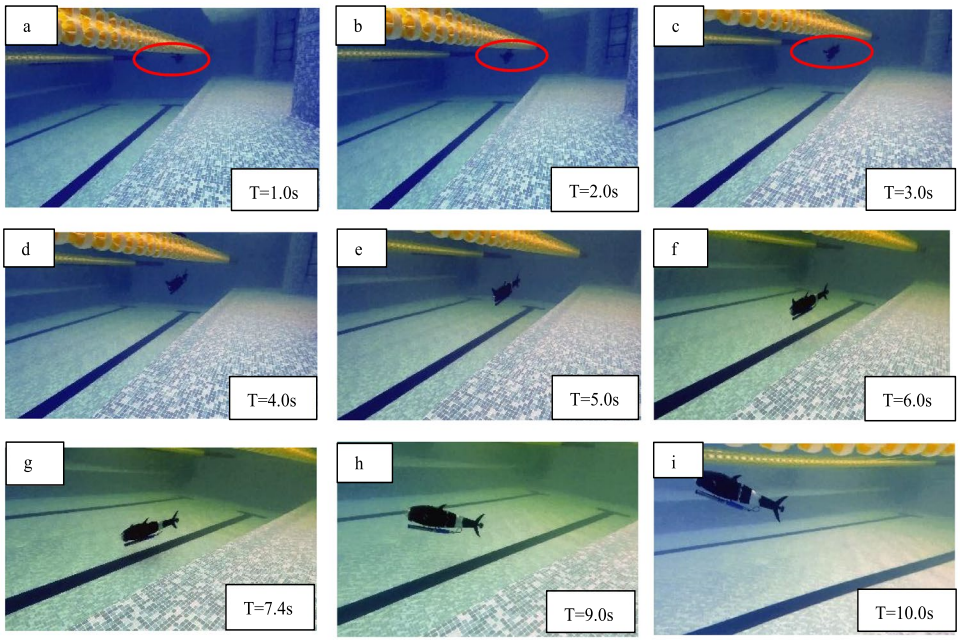


(a)

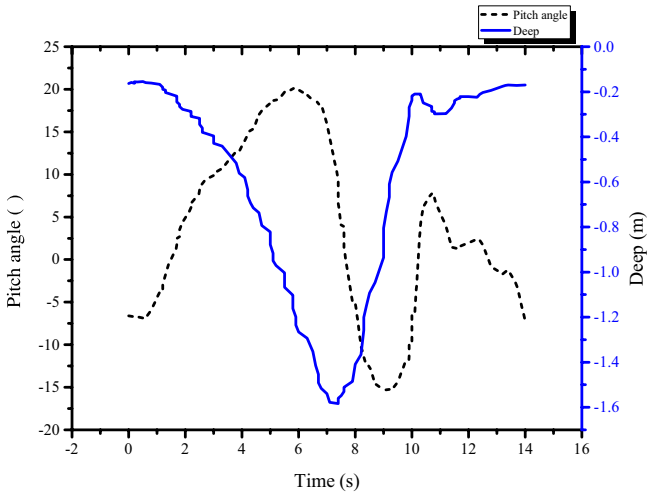


(b)

**Fig. 8** Submerging/ascending tests of the robotic fish. **a** Snapshot of the diving and surfacing motions, **b** pitch angle and depth change data during surfacing and diving


Robotic fish

(a)

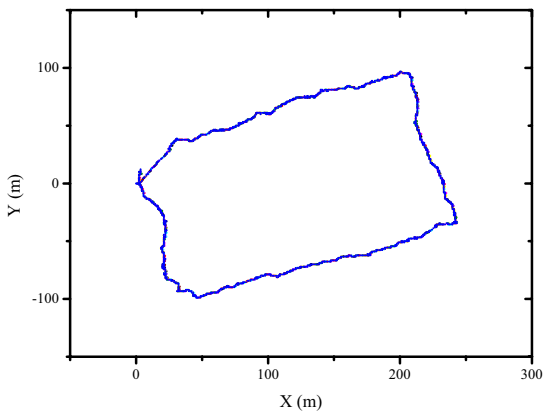
100
0
-100
Y (m)
0
100
200
300
X (m)

(b)

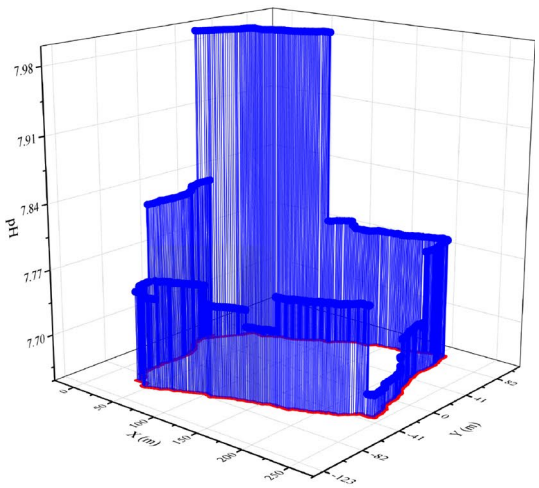
7.98
7.91
7.84
7.77
7.70
pH
X (m)
Y (m)

(d)

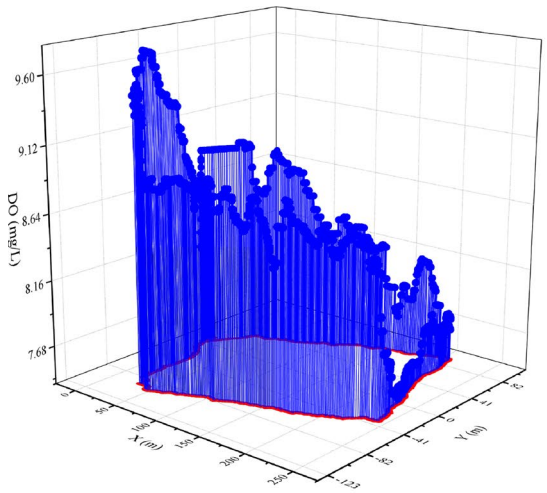
9.60
9.12
8.64
8.16
7.68
DO (mg/L)
X (m)
Y (m)

(c)

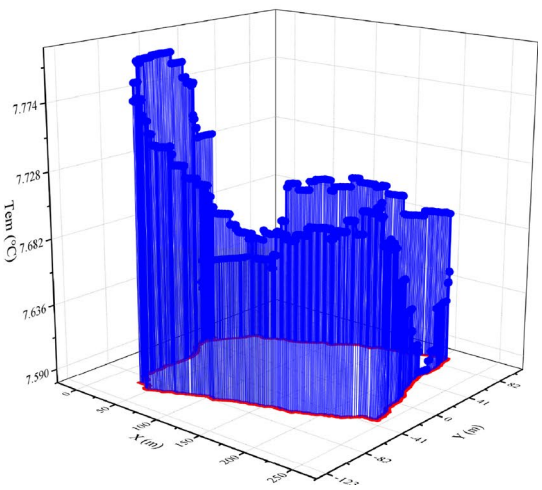
7.774
7.728
7.682
7.636
7.590
Tem (°C)
X (m)
Y (m)

(e)

◂**Fig. 9** Experiment of the water quality monitoring. **a** Experimental scene of the water quality monitoring, **b** the trajectory of the robotic fish around the breeding pond, **c** changes in the dissolved oxygen value in breeding pond, **d** changes in the PH value of breeding pond, **e** changes in the temperature value of the breeding pond

### 4.5 Field Experiments on Water Quality Monitoring

In order to examine the monitoring performance of the developed robotic fish, some field tests of water quality monitoring were carried out in the breeding ponds of farmers in Jiangsu Province, China in January 2022. The breeding ponds was close to Taihu Lake and Ge Lake, with intertwined rivers, dense ponds and rich aquatic resources. It is a major aquaculture market in southern Jiangsu. Therefore, water quality monitoring has received special attention. The experimental scene of the water quality monitoring is shown in Fig. 9a. In this experiment, so as to monitor the growth of aquatic products, we used motorized robotic fish to acquire underwater data information, including dissolved oxygen value, pH value, temperature, and more. The robotic fish was ordered to drive in a predetermined area through the wireless communication module, collect relevant underwater data information, and transmit these data to the PC side in real time. With the help of the motion performance of the robot, all the data acquired by the field sensors were transmitted to the upper controller and displayed in real time, involving depth information from pressure sensor, the gesture information from the inertial sensor, location information from the GPS, and mostly critical underwater data information from the water quality multi-probe. According to the on-site monitoring of the farmer's breeding pool at the time, the dissolved oxygen value, pH value, and water temperature of the breeding pool water were approximately 8.46 mg/L, 7.79, and 7.7 °C, respectively. These data were also drawn into some dynamic curves that change over time to identify the trend of water quality over time. In addition, on-site data processing achieved fast water quality monitoring and is better than laboratory testing. Figure 9b shows swimming trajectory from GPS patrolling around the breeding pond. The dissolved oxygen, pH and temperature values were obtained in real time during the movement of the robotic fish, as shown in patrolling Fig. 9c–e, respectively. The success of field experiments indicates the mobility of robotic fish and the feasibility of robotic fish-based mobile water quality monitoring.

### 4.6 Discussion

The bionic robotic fish draws inspiration from nature, but it is higher than nature and has proven to be able to perform rapid and flexible exercise in a complex underwater environment. We have designed a new hybrid-drive bionic robotic fish that integrates high-speed and high-mobility features by integrating traditional propulsion technology and fish-like flexible drive technology. It has higher maneuverability compared to traditional propellers and faster swimming speed compared to fish-like propulsion robots. The above experimental results show that the propulsion mechanism of integrated swing and propeller can help machine fish work effectively. In this study, our newly developed hybrid-drive bionic robotic fish achieves better performance in forward swimming speeds, turning rates, submerging or ascending. Our experimental results indicate that a hybrid-drive bionic robotic fish can achieve fast swimming and maneuverability with relatively high probability on the same robotic platform. What is more, using the robotic fish as a platform, it is equipped with a variety of high-precision sensing equipment including GPS pressure sensors and multiple water quality sensors to achieve swimming pool testing and field testing.

Despite the successful implementation of the monitoring of the real world, there are still some limitations for the developed machine fish. First, the design of robotic fish needs to comprehensively consider its own swimming speed and turning performance in order to better complete tasks such as water quality monitoring. In nature, real fish not only have a swimming speed of about 2.5–4 BL/s, but also can achieve turns of less than 0.2 BL [27]. Biotelemetry was used to examine the swimming behavior of Pacific bluefin tuna in cages, and the burst and steady swim speeds were estimated to be 5.2 and 1.1 BL/s [28], respectively, based on the frequency of tail beats.The movement parameters of yellow fin tuna schools were analyzed by means of scanning sonar in tuna purse seine capture situations in the Oman Sea, and the swimming speed ranged from 1.19 to 4.42 m/s [29]. However, there is still a certain gap between our tuna sports performance and real fish, and the robotic fish designed in this paper still has a lot of room for improvement. Secondly, although multiple water quality sensors are installed externally for easy replacement, it is unavoidable to have a certain negative impact on hydrodynamic performance. Therefore, internal mounting may be a better way to reduce drag. In addition, in the field test, the communication signal between the wireless communication module and the PC terminal is weak and extremely unstable; and the GPS signal also takes a long time to obtain the signal due to the cover of the fish cover. In the design of the later mechanical structure, these two parts need to be designed separately on the back of the fish, so that the signal is stable and easier to send and receive. Finally, the GPS positioning can be combined with the inertial sensor calculation to realize the three-dimensional positioning of the robotic fish. Therefore, we will consider

improving the communication capabilities of the next generation of robotic fish.

## 5 Conclusions and Future Work

This paper proposed a mechanical design scheme of robotic fish for water quality monitoring. It was first proposed to be driven by pectoral fins, waist and tail double joints (BCF) and propellers to achieve bending, twisting and 3D maneuvering performance. Unlike traditional rubber-made bionic fish skin and glue sealants, we designed a hard pressure housing made from dynamic sealing to enhance the adaptability and safety of robotic merpeople in the wild. To test the multi-modal movement performance of the robotic fish, we conducted tests such as forward swimming, turning, and diving/ascending in the swimming pool. The maximum propulsion speed of the robotic fish can achieve about 1.16 m/s (about 1 BL/s), and its minimum turning radius was 0.53 m (about 0.46 BL), and its maximum turning speed can reach 78.6 °/s. The diving depth of the robotic fish was about 1.4 m, and the lowest depth was reached in about 7 s, which can realize three-dimensional movement. Finally, the field water quality monitoring experiment had completed the circle inspection of water quality parameters. At the same time, the quality monitoring of the breeding pond had proved the great feasibility and potential of the robotic fish. The ongoing and future work will concentrate on the intelligent control of robotic fish to autonomously monitor waters and plan swimming paths based on assigned tasks and complex underwater environments. In addition, we will equip the robotic fish with edge computing modules and vision systems to analyze and process underwater images in real time.

**Supplementary Information** The results supporting this study can be found in the experimental video in Supplementary Materials to this paper.

**Supplementary Information** The online version contains supplementary material available at https://doi.org/10.1007/s42235-022-00282-1.

**Acknowledgements** This work was supported by the National Key R&D Program of China (2022YFE0107100), the National Key R&D Programs of China (Grant No. 2019YFD0901000), and the National Natural Science Foundation of China (Grant No. 61903007).

**Data Availability Statement** The data generated during and/or analysed during the current study are available from the author on reasonable request.

## Declarations

**Conflict of interest** All authors declare that they have no conflict of interest.

## References

1. Roper, D., Harris, C. A., Salavasidis, G., Pebody, M., Templeton, R., Prampart, T., et al. (2021). Autosub long range 6000: A multiple-month endurance AUV for deep-ocean monitoring and survey. *IEEE Journal of Oceanic Engineering, 46,* 1179–1191.
2. Honaryar, A., & Ghiasi, M. (2018). Design of a bio-inspired hull shape for an AUV from hydrodynamic stability point of view through experiment and numerical analysis. *Journal of Bionic Engineering, 15,* 950–959.
3. Sfakiotakis, M., Lane, D. M., & Davies, J. B. C. (1999). Review of fish swimming modes for aquatic locomotion. *IEEE Journal of Oceanic Engineering, 24*, 237–252.
4. Xie, F. R., Zuo, Q. Y., Chen, Q. L., Fang, H. T., He, K., Du, R. X., et al. (2021). Designs of the biomimetic robotic fishes performing body and/or caudal fin (BCF) swimming locomotion: A review. *Journal of Intelligent and Robotic Systems, 102,* 1.
5. Stefanini, C., Orofino, S., Manfredi, L., Mintchev, S., Marrazza, S., Assaf, T., Capantini, L., Sinibaldi, E., Grillner, S., Wallen, P., & Dario, P. (2012). A compliant bioinspired swimming robot with neuro-inspired control and autonomous behavior. *IEEE International Conference on Robotics and Automation, 2012*, 5094–5098.
6. Zhong, Y., Li, Z., & Du, R. X. (2017). A novel robot fish with wire-driven active body and compliant tail. *IEEE/ASME Transactions on Mechatronics, 22*, 1633–1643.
7. Clapham, R. J., & Hu, H. S. (2014). iSplash-II: Realizing fast carangiform swimming to outperform a real fish. *IEEE/RSJ International Conference on Intelligent Robots and Systems, 2014,* 1080–1086.
8. Zhu, J., White, C., Wainwright, D. K., Di Santo, V., Lauder, G. V., & Bart-Smith, H. (2019). Tuna robotics: A high-frequency experimental platform exploring the performance space of swimming fishes. *Science Robotics, 4*(34), 1.
9. White, C. H., Lauder, G. V., & Bart-Smith, H. (2020). Tunabot flex: A tuna-inspired robot with body flexibility improves high-performance swimming. *Bioinspiration and Biomimetics, 16,* 026019.
10. Du, S., Wu, Z. X., & Yu, J. Z. (2019). Design and yaw control of a two-motor-actuated biomimetic robotic fish. *IEEE International Conference on Robotics and Biomimetics (ROBIO), 2019*, 126–131.
11. Liao, P., Zhang, S. W., & Sun, D. (2018). A dual caudal-fin miniature robotic fish with an integrated oscillation and jet propulsive mechanism. *Bioinspiration and Biomimetics, 13,* 1.
12. Liang, J. H., Zheng, W. F., Wen, L., Wang, T. M., & Xie, C. Y. (2009). Propulsive and maneuvering performance of two joints biorobotic autonomous undersea vehicle SPC-III. In *IEEE international conference on robotics and Biomimetics* (pp. 314–320).
13. Clark, A. J., Tan, X. B., & Mckinley, P. K. (2015). Evolutionary multiobjective design of a flexible caudal fin for robotic fish. *Bioinspiration and Biomimetics, 10,* 1.
14. Shen, F., Wei, C. M., Cao, Z. Q., Zhou, C., Xu, D., & Zhang, W. Y. (2011). Water quality monitoring system based on robotic dolphin. In *2011 9th world congress on intelligent control and automation* (pp. 243–247).
15. Ryuh, Y. S., Yang, G. H., Liu, J. D., & Hu, H. S. (2015). A school of robotic fish for mariculture monitoring in the sea coast. *Journal of Bionic Engineering, 12*, 37–46.
16. Zhang, F. T., En-Nasr, O., Litchman, E., & Tan, X. B. (2015). Autonomous sampling of water columns using gliding robotic fish: Control algorithms and field experiments. *IEEE International Conference on Robotics and Automation, 2015*, 517–522.
17. Wu, Z. X., Liu, J. C., Yu, J. Z., & Fang, H. (2017). Development of a novel robotic dolphin and its application to water quality

monitoring. *IEEE/ASME Transactions on Mechatronics, 22*, 2130–2140.
18. Conry, M., Keefe, A., Ober, W., Rufo, M., & Shane, D. (2013). BIOSwimmer: Enabling technology for port security. *IEEE International Conference on Technologies for Homeland Security (HST), 2013,* 364–368.
19. Buck, J., Cavalcanti, G., Mandel, P., Schumacher, E., & Shiplett, S. B. (2009). GhostSwimmer, A Biometric Robotic Fish (Boston Engineering).
20. Ellington, C. P. (1999). The novel aerodynamics of insect flight: Applications to micro-air vehicles. *Journal of Experimental Biology, 202*, 3439–3448.
21. Matta, A., Pendar, H., Battaglia, F., & Bayandor, J. (2020). Impact of caudal fin shape on thrust production of a thunniform swimmer. *Journal of Bionic Engineering, 17*, 254–269.
22. Liu, J. D., & Hu, H. S. (2010). Biological inspiration: From carangiform fish to multi-joint robotic fish. *Journal of Bionic Engineering, 7*, 35–48.
23. Su, Z. S., Yu, J. Z., Tan, M., & Zhang, J. W. (2014). Implementing flexible and fast turning maneuvers of a multijoint robotic fish. *IEEE-ASME Transactions on Mechatronics, 19,* 329–338.
24. Yu, J. Z., Liu, L. Z., Wang, L., Tan, M., & Xu, D. (2008). Turning control of a multilink biomimetic robotic fish. *IEEE Transactions on Robotics, 24*, 201–206.
25. Du, S., Wu, Z. X., Wang, J., Qi, S. W., & Yu, J. Z. (2021). Design and control of a two-motor-actuated tuna-inspired robot system. *IEEE Transactions on Systems, Man, and Cybernetics: Systems, 51*, 4670–4680.
26. Yu, J. Z., Liu, J. C., Wu, Z. X., & Fang, H. (2018). Depth control of a bioinspired robotic dolphin based on sliding mode fuzzy control method. *IEEE Transactions on Industrial Electronics, 65*, 2429–2438.
27. Dickinson, M. H., Farley, C. T., Full, R. J., Koehl, M. A. R., Kram, R., & Lehman, S. (2000). How animals move: An integrative view. *Science, 288,* 100–106.
28. Susumu, O., Yasushi, M., Wataru, S., & Hidemi, K. (2006). Study on swimming behavior of cultured pacific bluefin tuna using biotelemetry. *Memoirs of the Faculty of Agriculture of Kinki University, 39*, 79–82.
29. Hosseini, S. A., & Ehsani, E. (2014). An investigation of reactive behavior of yellowfin tuna schools to the purse seining process. *Iranian Journal of Fisheries Sciences, 13*, 330–340.